Deciphering the role of southern gateways and carbon dioxide on the onset of the Antarctic Circumpolar Current

Vincent Lefebvre, Yannick Donnadieu, Pierre Sepulchre, Didier Swingedouw, Zhong-Shi Zhang

Deciphering the role of southern gateways and carbon dioxide on the onset of the Antarctic Circumpolar Current

Vincent Lefebvre,[1] Yannick Donnadieu,[1] Pierre Sepulchre,[1] Didier Swingedouw,[1] and Zhong-Shi Zhang[2]

Received 15 May 2012; revised 31 August 2012; accepted 3 September 2012; published 11 October 2012.

[1] Growth of Antarctic ice sheet during the Cenozoic 34 million years ago appears as a potential tipping point in the long term cooling trend that began 50 Ma ago. For decades, the onset of the Antarctic Circumpolar Current (ACC) following the opening of the Drake Passage and of the Tasman Seaway has been suggested as the main driver of the continental-scale Antarctic glaciation. However, recent modeling works emphasized that the Eocene/Oligocene atmospheric carbon dioxide (CO_2) lowering could be the primary forcing of the Antarctic glaciation, questioning the ACC theory. Here, we investigate the response of the ACC to changes in CO_2 concentrations occurring from the late Eocene to the late Oligocene. We used a fully coupled atmosphere-ocean model (FOAM) with a mid-Oligocene geography. We find that the opening of southern oceanic gateways does not trigger the onset of the ACC for CO_2 typical of the late Eocene (>840 ppm). A cooler background climatic state such as the one prevalent at the end of the Oligocene is required to simulate a well-developed ACC. In this cold configuration, the intensified sea-ice development around Antarctica and the resulting brine formation lead to a strong latitudinal density gradient in the Southern Ocean favoring the compensation of the Ekman transport, and consequently the ACC. Our results imply that the ACC has acted as a feedback rather than as a driver of the global cooling.

Citation: Lefebvre, V., Y. Donnadieu, P. Sepulchre, D. Swingedouw, and Z.-S. Zhang (2012), Deciphering the role of southern gateways and carbon dioxide on the onset of the Antarctic Circumpolar Current, *Paleoceanography*, *27*, PA4201, doi:10.1029/2012PA002345.

1. Introduction

[2] The ACC is a strong circumpolar oceanic current responsible for the thermal isolation of the Antarctic from the tropical waters [*Kennett*, 1977; *Toggweiler and Bjornsson*, 2000]. The development of this current is only made possible by the evolution of the continental configuration which results in the opening of the Drake Passage (DP) between Antarctica and South America around 50 Ma [*Lagabrielle et al.*, 2009, and references therein] and of the Tasman gateway (with a sufficient deepening at around 33 Ma) separating Antarctica and Australia at 35 Ma [*Stickley et al.*, 2004]. Drake Passage had a complex history of opening [*Lagabrielle et al.*, 2009] and the timing of the ACC onset is not clearly established [*Barker and Thomas*, 2004], but the synchronicity of this tectonics feature with the first records indicating the presence of an ice sheet over Antarctica [*Ehrmann and Mackensen*, 1992; *Wilson et al.*, 1998; *Zachos et al.*, 1999, 2001] has long led scientists to consider the ACC onset as the trigger of ice inception over this continent at 34 Ma [*Kennett et al.*, 1974; *Livermore et al.*, 2005; *Murphy and Kennett*, 1986; *Zachos et al.*, 1996].

[3] A great amount of studies using GCMs have assessed the effect of the ACC on the Antarctica thermal isolation by modifying the configuration of the gateways (DP or Tasman gateway) of a present-day geography [*Mikolajewicz et al.*, 1993; *Nong et al.*, 2000; *Sijp and England*, 2004, 2005; *Sijp et al.*, 2009], an idealized geography [*Toggweiler and Bjornsson*, 2000], or an Eocene geography [*Huber and Sloan*, 2001; *Huber and Nof*, 2006; *Huber et al.*, 2003, 2004; *Zhang et al.*, 2010; *Sijp et al.*, 2011]. *Sijp and England* [2004] find a warmer southern hemisphere surface air temperature when the DP is closed in the present-day geography suggesting that the opening of this later may have contributed to the glaciation of Antarctica. In the continuity, *Sijp et al.* [2009] studied the influence of a high CO_2 concentration and of the open/closed DP configuration on the climate accounting for the present-day geography. They find that the closure of the DP cools the deep ocean temperature and Antarctic SST and that the magnitude of this cooling increases with increasing CO_2. However, the Eocene-Oligocene continental configuration is different of the modern one and *Zhang et al.* [2010], using the same GCM than in the present study, concluded that the climate effect of

[1]Laboratoire des Sciences du Climat et de l'Environnement CEA-CNRS, CEA Saclay, Gif-sur-Yvette, France.
[2]Bjerknes Centre for Climate Research, UniResearch, Bergen, Norway.

Corresponding author: V. Lefebvre, Laboratoire des Sciences du Climat et de l'Environnement CEA-CNRS, CEA Saclay, Orme des Merisiers, FR-91190 Gif-sur-Yvette, France. (vincent.lefebvre@lsce.ipsl.fr)

0883-8305/12/2012PA002345

the DP on the Cenozoic cooling have been overestimated in the previous works using the modern geography. They demonstrated that the climate impact of the opening of the DP depends of the geometry of itself, which is different from the modern one during the Eocene. In the same way, *Huber and Sloan* [2001], *Huber and Nof* [2006], *Huber et al.* [2003, 2004] and *Sijp et al.* [2011] depicted the impact of the open/closed configuration of the Tasman gateway for an Eocene geography and found that the deepening of this gateway does not lead to a strong Antarctic cooling. More, *Huber and Nof* [2006] and *Sijp et al.* [2011] observed a warming of the East coast of Antarctica caused by the deepening of the Tasman gateway. They concluded that the opening and deepening of this seaway is unlikely to have caused the installation of the ice sheet on Antarctica at the Eocene-Oligocene boundary. As a synthesis, it appears that the opening of the southern gateways and the related initiation of the ACC is not the main forcing of the Cenozoic cooling and of the Antarctic glaciation favoring the CO_2 lowering as the main driver of this climatic perturbation. As well, simulations with atmospheric CO_2 concentrations lower than 2.5 PAL (one PAL stands for the Pre-industrial Atmospheric Level, *i.e.* 280 ppm) trigger the onset of an ice sheet on Antarctica [*DeConto and Pollard*, 2003]. Recent records showing a lowering of the atmospheric CO_2 concentrations at ca 35 Ma [*Pagani et al.*, 2005, 2011] support these last results. However, no study attempts to depict the sensitivity of the ACC as a function of the CO_2 atmospheric level, and consequently of the climate cooling, during the Oligocene period. In order to fill this gap and to provide further constraints on our understanding of the mechanisms and feedbacks associated with the Cenozoic cooling, we used a fully coupled ocean-atmosphere model (FOAM) with an Oligocene geography, an ice-free Antarctic continent and an opened seaways configuration to depict the influence of the climate state induced by CO_2 changes on the ACC. Rather than opposing the two mechanisms traditionally evoked (ACC versus CO_2 lowering), we want to emphasize here that they may have been linked. Indeed, it is generally implied that the ACC initiation during the Cenozoic was only prevented by the closed gateways of the Austral Ocean. The opening of these gateways occurs in the early Oligocene characterized by CO_2 levels 2 to 4 times higher than the pre-industrial level [*Pagani et al.*, 2005, 2011] and representative of a warmer climate than today without ice sheet over Antarctica [*Zachos et al.*, 2001]. However, the modern ACC exists in a low CO_2 world (an icehouse world, with respect to the geological record) characterized by the presence of a continental-scale ice sheet over Antarctica and the efficiency of this current in a warmer world (i.e., during the early Oligocene) remains undefined.

2. Methods

2.1. Model Description

[4] The model used here is the FOAM (Fast Ocean Atmosphere Model) Atmosphere-Ocean General Circulation Model. The atmospheric component of FOAM is a parallelized version of NCAR's Community Climate Model 2 (CCM2) with the upgraded radiative and hydrologic physics incorporated in CCM3 v. 3.2 [*Kiehl et al.*, 1996]. The atmosphere runs at R15 spectral resolution (4.5° × 7.5°) with 18 levels. The ocean component of FOAM, the Ocean Model version 3 (OM3), is a z-coordinate ocean model that has been optimized for performance and scalability on parallel computers [*Jacob*, 1997]. OM3 is dynamically similar to the GFDL Modular Ocean Model (MOM) and contains 24 vertical layers, a 128 × 128 grid (1.4° × 2.8°) and uses simple second order differencing and a fully explicit time step scheme for the barotropic and baroclinic modes. The ocean and atmospheric models are linked by a coupler, which implements the land and sea ice models CSIM 2.2.6 [*Bettge et al.*, 1996] and calculates and interpolates the fluxes of heat and momentum between the atmosphere and ocean models [*Jacob*, 1997]. The sea ice component in this FOAM version (1.5) uses the thermodynamic component of the sea-ice model in CSM1.4 [*Weatherly et al.*, 1998], which is based on the Semtner 3-layer thermodynamics snow/ice model [*Semtner*, 1976; *Bettge et al.*, 1996]. The FOAM model has been widely used in paleoclimate studies [*Poulsen and Jacob*, 2004; *Donnadieu et al.*, 2009; *Zhang et al.*, 2010, *Dera and Donnadieu*, 2012].

2.2. Experimental Design

[5] The CO_2 level throughout the Eocene and the Oligocene is estimated to vary from around 3–4 PAL during the late Eocene-early Oligocene to ca. 1 PAL at the end of this epoch [*Pagani et al.*, 2005, 2011]. Both boron-isotope and alkenones depict CO_2 concentrations falling from 1000 ppm to around 700 ppm at the Eocene-Oligocene boundary, a change consistent with model estimates for the threshold in CO_2 level required for Antarctic glaciation (2.5 PAL) [*DeConto and Pollard*, 2003]. To capture this range of variation, we performed a set of simulations at various CO_2 concentrations (1, 1.5, 2, 2.5 and 3 PAL) to characterize the influence of this greenhouse gas-induced climate on the ACC during the Oligocene. These simulations are called Dop (Drake open) followed by the CO_2 level in PAL (e.g., Dop-1x). A FOAM simulation (CTRL-1x) considering the present-day geography (topography and bathymetry) and a 1 PAL CO_2 level is used as a control to describe the way the ACC is simulated (Table 1).

[6] We used the same method and data as introduced by *Zhang et al.* [2010] to reconstruct the middle Oligocene geography (Figure 1) in our Dop simulations. The latter is designed following the paleogeography of *Scotese* [2001] and paleobathymetry is estimated using the method outlined by *Bice et al.* [1998]. The paleogeography includes the reconstructions of mountains, coastlines and shallow ocean basin, as well as magnetic lines on the ocean floor. The coastlines for the Tethys seaway are modified according to the paleogeography map of *Barrier and Vrielynck* [2008]. The coastlines for the Central American seaway are set according to the reconstruction by *Iturralde-Vinent and MacPhee* [1999]. The age-depth relationships established by *Bice et al.* [1998] are used to calculate the depth of each magnetic line. Finally, this depth data is interpolated into a global area configuration. In this reconstructed geography, the Drake and Tasman gateways are open. The topography over the Antarctic does not exceed 2000 m and we prescribed a tundra albedo on this continent. By contrast to the present-day configuration, Australia is at a southern position close to the Antarctic and South America is located at the same position as today. The Panama seaway is open and the Tethys

Table 1. Boundary Conditions (CO_2 and Antarctic Ice Sheet), Current Intensity in the Gateways, Density Gradient Between 45° and 65°S (Zonally and Depth-Averaged, 0–1500 m), and Global Surface Air Temperature

Simulations	CO_2 (ppm)	Antarctic Ice Sheet Prescribed	Drake Current (Sv)	Tasman Current (Sv)	Density Gradient ($kg.m^{-3}$)	Global Surface Air Temperature (°C)
Dop-1x	280	No	89	89	0.3	13.2
Dop-1.5x	420	No	57	64	0.23	15.4
Dop-2x	560	No	31	45	0.19	16.6
Dop-2.5x	700	No	9	15	0.13	18.1
Dop-3x	840	No	10	16	0.13	19
CTRL-1x	280	Yes	113	136	0.39	14.2

connects the Atlantic and Indian oceans. The Atlantic Ocean is also more constricted than today. Simulations have been run for 1000 years and we consider the average over the last 50 years as a steady state for each simulation. Figure 2 depicts the evolution of the ocean temperature during the 1000 simulated years for the Dop simulations. We consider that the steady state is reached after 800 simulated years.

3. Results and Discussion

3.1. The ACC in the Control Simulation

[7] The CTRL-1x simulation simulates the ACC well compared to the observations and the IPCC-AR4 coupled model control simulation. The zonal transport values for the modern simulation falls within the range of present-day values estimated at 95 +/− 2 Sv in the upper 1000 m [*Firing et al.*, 2011], 107.3 +/− 10.4 Sv above 3000 m [*Cunningham et al.*, 2003], and 134 Sv [*Whitworth and Peterson*, 1985] to 154 +/− 38 Sv [*Firing et al.*, 2011] for the entire water column. *Russell et al.* [2006] provided an intercomparison of IPCC-AR4 (Intergovernmental Panel on Climate Change's Fourth Assessment Report) coupled-model control simulations focusing on the southern ocean. We compare here the ACC transport, the latitude of maximum wind stress and the density gradient of the FOAM CTRL-1X simulation to the values compiled by *Russell et al.* [2006] for 18 IPCC model results (Table 2). Based on these results, FOAM is affiliated to a group (Table 2) of simulations characterized by an equatorward displacement of peak wind stress, a density gradient weaker than the observation and a stronger maximum wind stress (Max τ_x). This group contains the models that approach the observation and the GFDL-CM2.1 control simulation that provides the best correspondence with the observations. As a result FOAM appears to be a good tool, in the average of the IPCC AR4 models, to study the Southern Ocean and depict the variation of the ACC in response to the CO_2 level. For example, FOAM belongs to the same group as MIROC3.2 (hires), GFDL-CM2.0, BCCR-BCM2.0, MRI-CGCM2.3.2a and both CCMA models.

3.2. The ACC in the Oligocene Simulations

[8] Surprisingly, we observe that the ACC, characterized by a strong eastward zonal current in the 1 and 1.5 PAL Dop simulations (as well as in the CTRL-1x), tends toward very low values when CO_2 increases (Figure 3). Zonal transport integrated over the water column at the Drake Passage

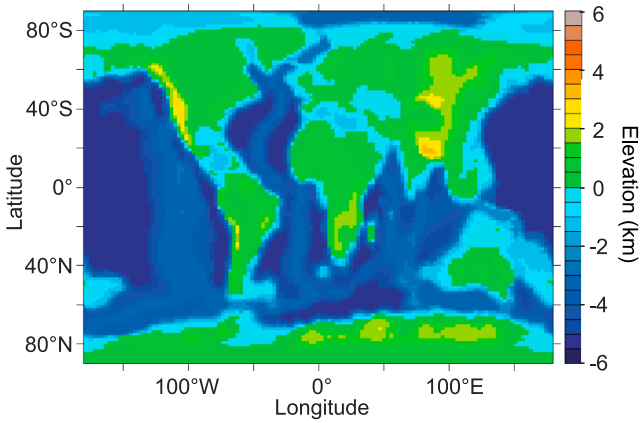

Figure 1. Oligocene reconstruction [*Zhang et al.*, 2010] used in the Dop simulations.

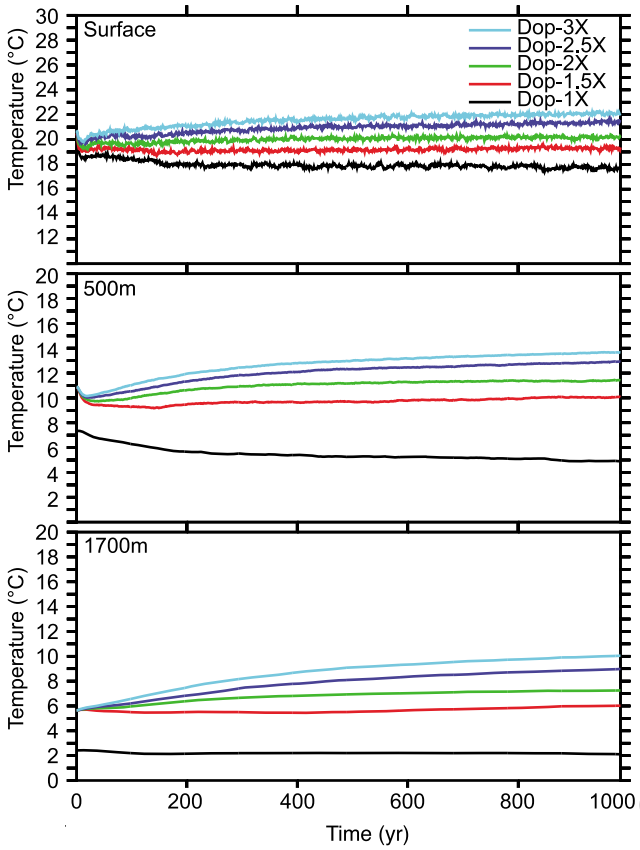

Figure 2. Evolution of the Ocean temperature (top) at the surface, (middle) 500 m and (bottom) 1700 m.

Table 2. Ocean and Atmosphere Characteristics Related to the ACC for 18 IPCC-AR4 Coupled Model Control Simulations Compared to the FOAM Control Simulation and Observation[a]

Model	ACC (Sv)	Lat. of Max τ_x (°S)	$\Delta\rho$ (kg.m^{-3})	Max τ_x (N.m^{-2})
Observation	135	52.4	0.58	0.161
GSIRO-Mk3.0	336	51.3	0.85	0.207
GISS-ER	266	46	0.62	0.107
UKMO-HadCM3	223	51.3	0.97	0.163
GISS-AOM	202	43.5	0.38	0.166
UKMO-HadGEM1	199	52.25	0.65	0.190
MIROC3.2 (medres)	190	46	0.43	0.184
GFDL-CM2.1	135	51	0.58	0.162
MIROC3.2 (hires)	125	46.5	0.49	0.175
GFDL-CM2.0	113	46	0.56	0.149
FOAM CTRL-1X	113	46.2	0.37	0.172
CCCMA-CGCM3.1 (T63)	106	48.8	0.43	0.192
BCCR-BCM2.0	105	48.8	0.53	NA
MRI-CGCM2.3.2a	94	48.8	0.4	0.157
CCCMA-CGCM3.1 (T47)	93	46.4	0.27	0.180
INM-CM3.0	80	48	0.71	0.172
IAP-FGOALS1.0g	75	48.8	0.39	0.138
CNRM-CM3	54	46	0.31	0.106
IPSL-CM4	34	41.8	0.18	0.160
GISS-EH	−6	46	0.43	0.096

[a]ACC transport is calculated in the Drake Passage, Lat of max τ_x is the latitude of the maximum zonally averaged wind stress, the density difference $\Delta\rho$ correspond to the zonal and depth-averaged (0–1500 m) difference of density between 65°S and 45°S. Reference: *Russell et al.* [2006].

longitude confirms this trend. For CO_2 values greater than or equal to 2.5 PAL, the zonal transport remains constant at low values around 10 Sv (10^6 m^3/s). When CO_2 concentration falls from 2 to 1 PAL (global air temperature decreases from 16.6 to 13.2°C), the strength of the zonal transport increases from 30 to 90 Sv (Table 1). Although the geography and bathymetry show substantial difference between the Oligocene and control configurations, the values calculated in the Dop-1x simulation (89 Sv) and in the CTRL-1x simulation (113 Sv) are on the same order. Zonal transport integrated over the water column at the Tasman gateway latitudes follows the same trend and also becomes weaker when CO_2 exceeds 2 PAL (around 10 Sv, Table 1). The ACC is found throughout the whole water column from the surface to the seafloor (the depth of the seafloor is at 2100 m in our reconstruction, while its present-day average depth reaches 3500 m) at 1 PAL (Figure 4). The depth-profile of the current is similar in the Dop-1x and CTRL-1x simulations for the first 2000 m, suggesting that changes in geographical configuration between the Oligocene (opened gateways configuration) and the present-day have a weak influence on the ACC.

[9] There is no consensus on the prominent mechanism driving the ACC. Pressure gradient caused by bathymetry [*Munk and Palmen*, 1951], wind stress curl [*Stommel*, 1957], or buoyancy forcing [*Gent et al.*, 2001] are evoked as main

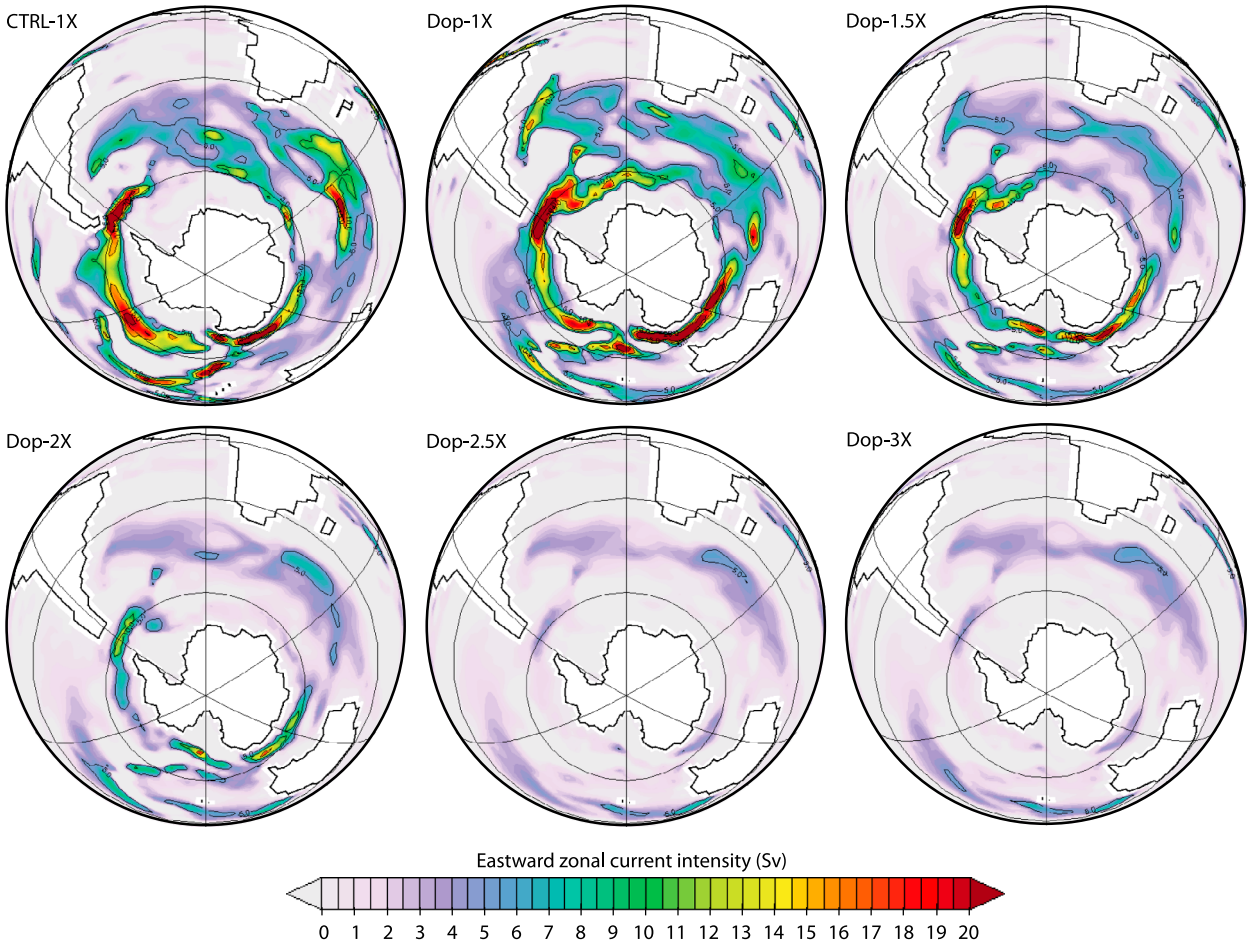

Figure 3. Eastward zonal transport integrated in depth (Sv).

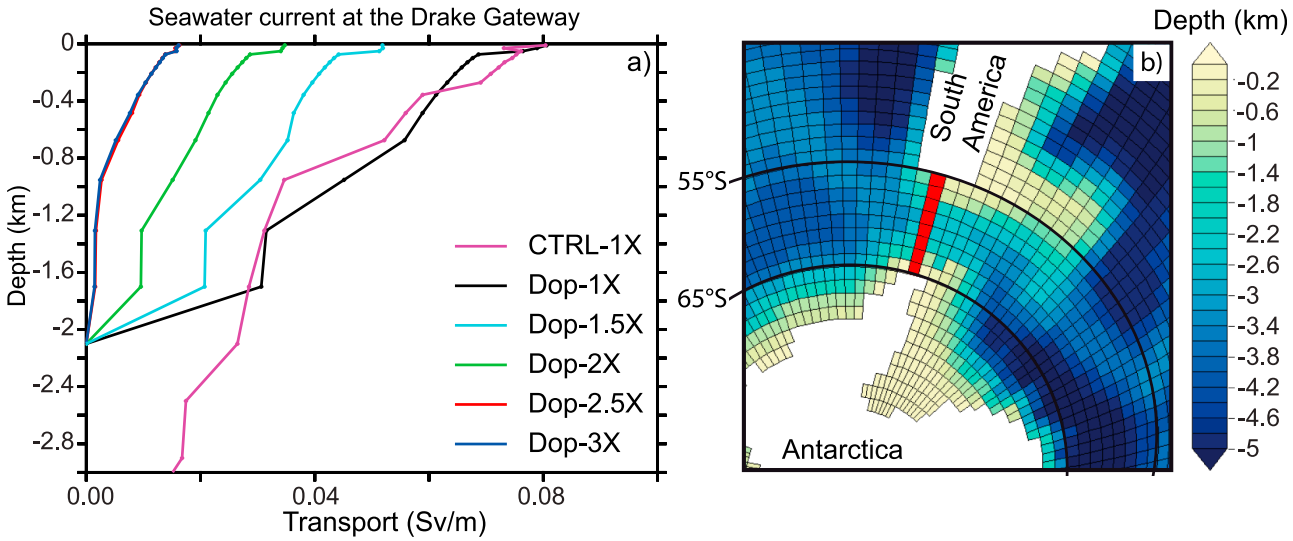

Figure 4. (a) Vertical profile of the transport (Sv/m) in each simulation. (b) The calculation of the current intensity is made on the red transect localized on the map.

contributors to the Southern Ocean dynamics. Several modeling studies concluded that the deep circulation in the Southern Hemisphere and the related modification of the density field as well as the vertical mixing coefficient could influence the ACC [*Cai and Baines*, 1996; *Gent et al.*, 2001]. However, available data fail to provide a definitive explanation.

[10] Theoretically, the weakening of the ACC can be caused by a diminution of the atmospheric driver, i.e., the Westerlies, or by a change in the oceanic meridional density gradient required to maintain this geostrophic current. Our Dop simulations show a very weak response of the strength and position of the Westerlies to the CO_2 increase (Figure 5a) with an increase in the mean latitudinal position of the maximal wind stress from 43.3°S at 1 PAL to 44.9°S at 3 PAL. This response seems to be in agreement with previous modeling studies that predict a poleward shift of the

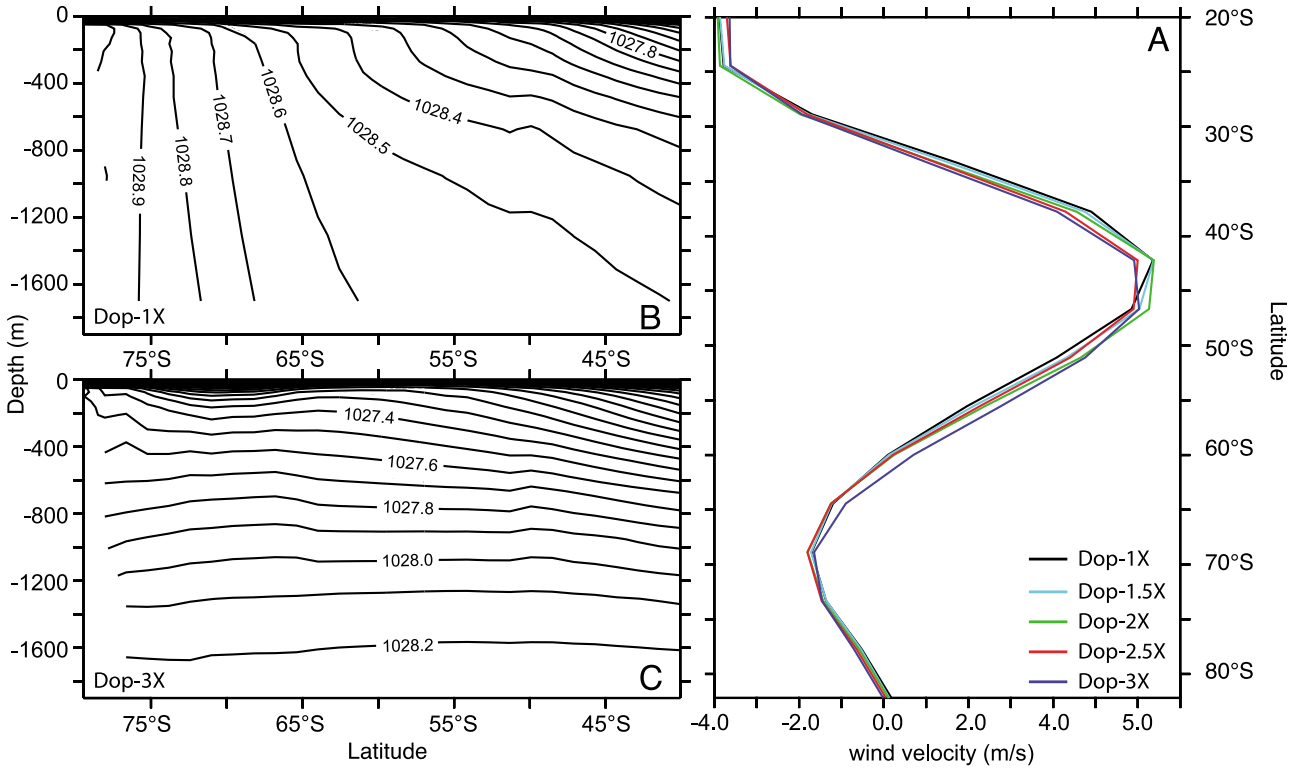

Figure 5. (a) Zonal averaged wind velocity for the Dop simulations. Averaged latitudinal profile of the density of seawater for the (b) Dop-1X and (c) Dop-3X simulations.

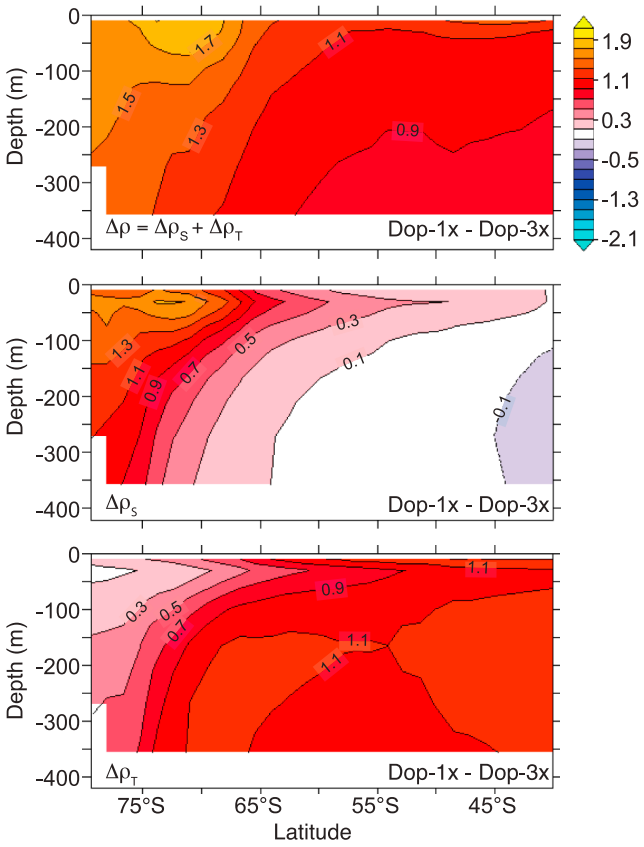

Figure 6. (top) Density difference between the Dop-1x and Dop-3x simulations and the density difference between the Dop-1x and Dop-3x simulations related to (middle) salinity and (bottom) temperature.

Westerlies in response to a global warming after the Last Glacial Maximum (LGM) [*Toggweiler et al.*, 2006]. However, the maximum poleward wind stress shift in our Dop 2.5 and 3 PAL simulations fails to explain the weakening of the ACC at high CO_2 concentrations, suggesting another forcing responsible for the observed weakening.

[11] However, our simulations show profound changes in the zonal-mean meridional density gradient of the Southern Ocean (Figures 5b and 5c). A highly stratified water column with a very weak latitudinal density gradient characterizes high CO_2 experiments, whereas the 1 PAL simulation shows a steep gradient, with denser waters poleward. The zonally and depth-averaged (0–1500 m) density difference between 65 and 45°S for each simulation reaches the highest value in the CTRL-1x simulation (0.37 kg.m^{-3}) and increases linearly in the Oligocene simulations from 0.13 at 2.5 and 3 PAL to 0.3 kg.m^{-3} at 1 PAL. The density difference between the Dop-1x and 3x simulations (Figure 6, top) is stronger at high latitude (1.3 to 1.7 at 65–70°S in the first 200 m deep).

[12] Temperature and salinity both influence the density. In order to distinguish their respective contribution, we linearize the density equation through the difference between Dop-1x and Dop-3x. The linearization ($\Delta\rho = \Delta\rho_S + \Delta\rho_T$ with $\Delta\rho_S = \beta\Delta S$ and $\Delta\rho_T = \alpha\Delta T$, where α is the thermal expansion and β is the haline contraction) leads a very weak residual between linearized and nonlinearized density differences (not shown). By analyzing the haline and thermal components, we notice that the salinity is the main contributor to our signal (Figure 6, middle). The difference from thermal component gradient is opposite to the density gradient (Figure 6, lower), illustrating that temperature dampens the density gradient initiated by salinity.

[13] The formation and melting of sea ice around Antarctica at 3 PAL is limited to the Weddell and the Ross Seas, while at 1 PAL, colder air temperatures allow sea ice to reach 55°S all around Antarctica (Figure 7). This leads to the formation of cold and saline deep waters through the effect of brine rejection during the process of sea-ice production. This deep water increases the meridional density gradient and thus the ACC. The onset of these two features is therefore intimately related as evoked in recent studies that suggest that the ACC is responsible for the modern vertical ocean structure [*Katz et al.*, 2011].

[14] However, uncertainties in the southern high-latitude sea ice and ocean response to climate perturbations are considerable [*Holland and Raphael*, 2006, *Roche et al.*, 2012]. The modern maximum sea ice area during the winter of the southern hemisphere (SIM) is estimated between 14.2 and 15.2 $\times$ 10^6 km^2 in September [*Gloersen et al.*, 1992] and the CTRL-1X simulation predicts a SIM equals to 16.5 $\times$ 10^6 km^2 (assuming a pre-industrial CO_2 level). As a result, FOAM provides a correct representation of the maximum sea ice coverage in winter (September) in the Southern Hemisphere for the control simulation, at least better than a lot of IPCC class model [cf. *Arzel et al.*, 2006]. The seasonality of the sea ice coverage in the CTRL-1X simulation differs from the observations in summer with a 0.2 $\times$ 10^6 km^2 minimum contrasting to 2 $\times$ 10^6 km^2 [*Gloersen et al.*, 1992] suggesting a stronger melting of the sea ice in FOAM during the summer of the Southern Hemisphere. While far from perfect, FOAM simulates correctly the modern day extent of the sea-ice cover in the Southern Hemisphere and seems therefore suitable for studying paleoclimate.

[15] In summary, our numerical experiments suggest that, in addition to the opening of oceanic gateways, the decrease in the CO_2 level during the Oligocene induces a sufficient cooling over the Southern Ocean to increase the sea-ice production and associated brine rejection. This would have resulted in saline and cold deep-water formation and would have increased the meridional density oceanic gradient allowing the activation of the ACC at around 30 Ma. Once this current is activated, the local cooling initiated by the thermal isolation of Antarctica may reinforce the deep-water formation and then the oceanic meridional gradient may act as a positive feedback loop, strengthening the stability of the Antarctic ice sheet.

[16] In our scenario, the ACC depends not only on the opening of the seaways but also on CO_2 forcing. Our Oligocene reconstruction favors the ACC since the seaways are wide and deep enough (2100 m) and localized at around 60°S. Therefore, the absence of the circumpolar current at high CO_2 levels cannot be explained by a geographic or bathymetric effect. Using the same GCM, *Zhang et al.* [2010] found that the ACC was weaker during the Eocene and at present-day in their high CO_2 (8 PAL) simulations. However, they only focused on the climatic impact of the seaways openings, but our results are consistent with their observations. Our results are also consistent with the conclusions of

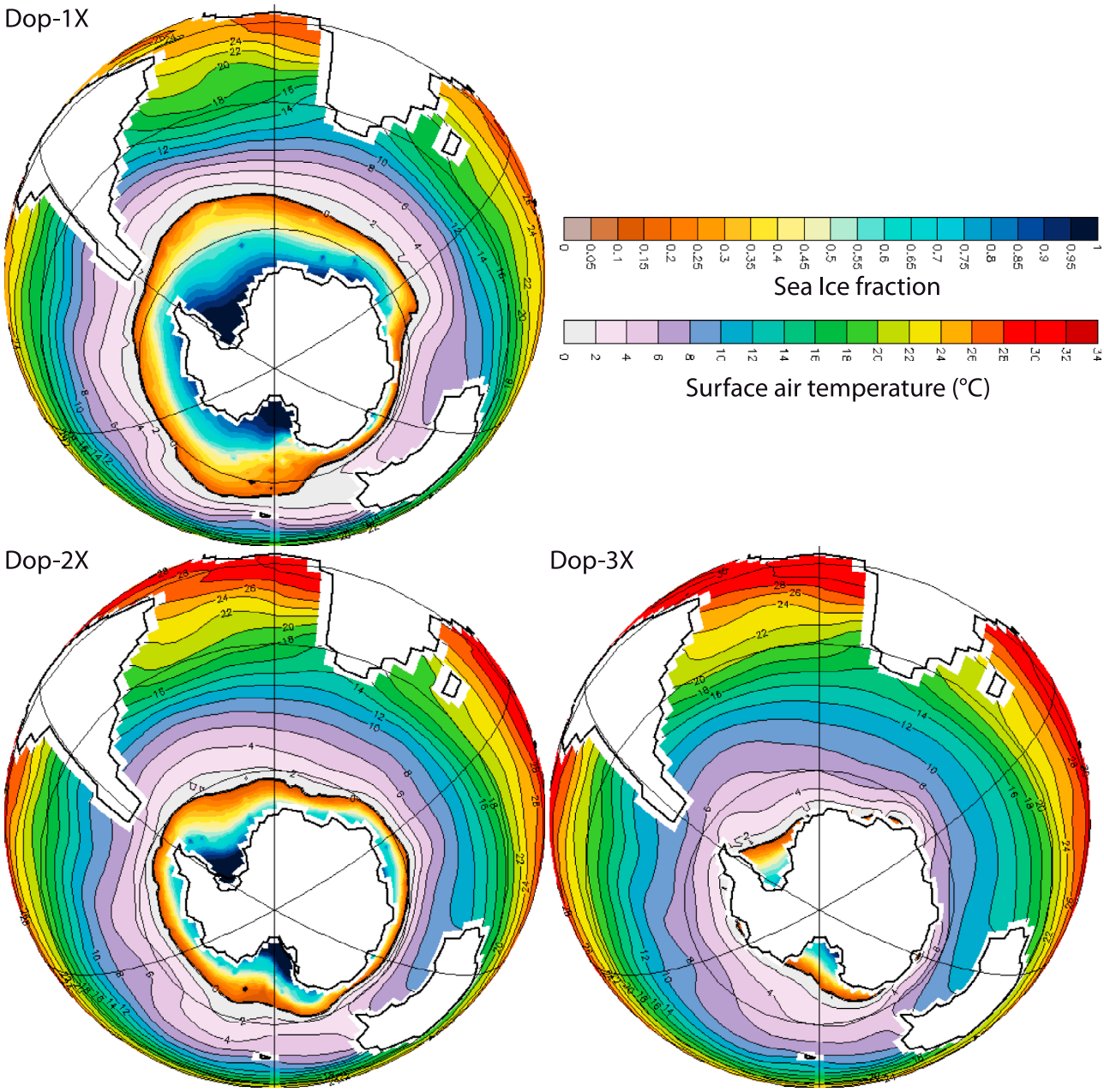

Figure 7. Sea ice fraction and surface air temperature during the austral winter season for the Dop-1x, Dop-2x and Dop-3x simulations.

Sijp et al. [2011] concerning the immaturity of the ACC with 1500 ppm of CO_2 that add further supports to our results. They are also in agreement with data constraining the evolution of the ACC such as sedimentological evidences [*Lyle et al.*, 2007] suggesting a Late Oligocene initiation of the ACC. *Lyle et al.* [2007] distinguish the existence of shallow water connections between the Atlantic and the Pacific in the Drake Passage region, as shown by the εNd isotope record in the middle Eocene [*Scher and Martin*, 2006, 2008], from the onset of an intense and deep circumpolar current that can only be tracked with evidence from the seafloor i.e., exchange of water between the Atlantic and Pacific as early as the middle Eocene, may be the consequence of shallow ocean currents. In contrast, the true ACC, characterized by a deep, intense current, did not develop until the end of the Oligocene. The increase in sortable silt mean size in the Tasman Gateway at 23.95 Ma [*Pfuhl and McCave*, 2005] confirms this theory. Our results shed light on these interpretations by providing the mechanism explaining the delay between the opening of gateways and the onset of the ACC.

[17] Our model simulates an ACC with modern intensity for an atmospheric CO_2 level of 1 PAL, a value which is not reached before the Late Oligocene in the CO_2 estimates based on the alkenones [*Pagani et al.*, 2005, 2011]. Following these CO_2 reconstructions, we find that the ACC began to increase between 31 and 28 Ma and may have

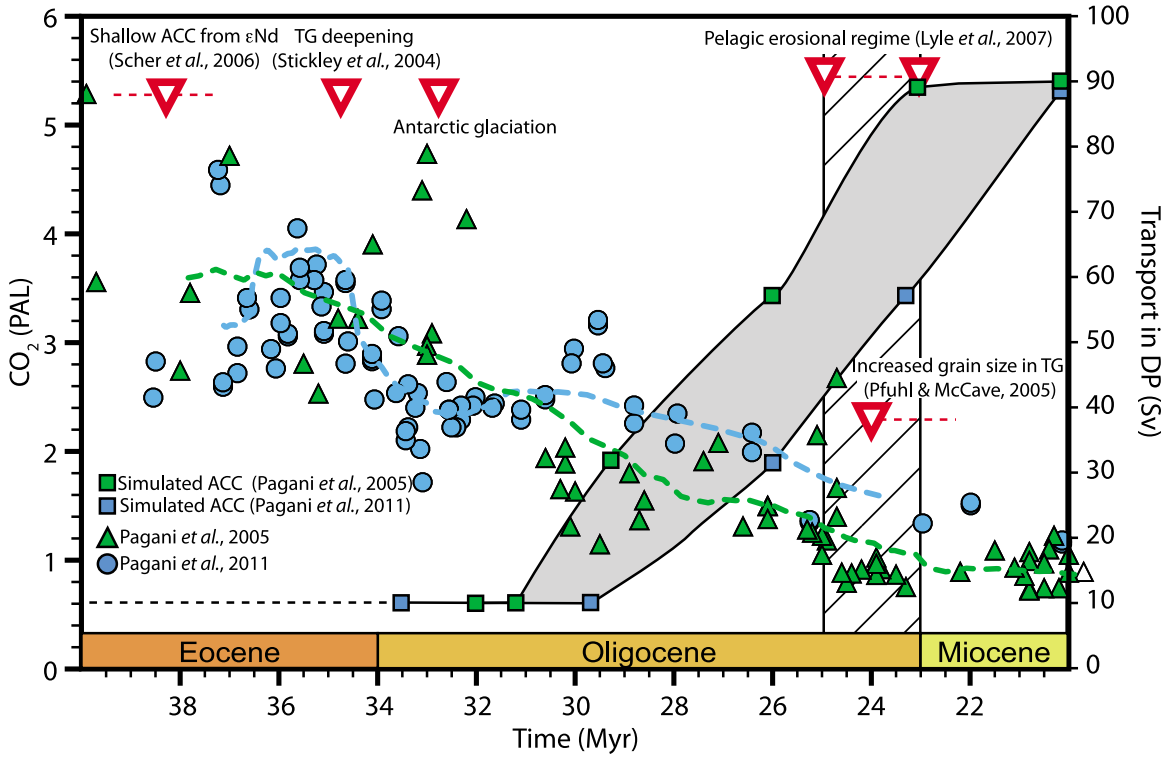

Figure 8. Evolution of the atmospheric CO_2 level deduced form alkenones and of the simulated transport of the ACC in the Drake Passage (DP) as a function of the 10 points smoothed curve from the data set of *Pagani et al.* [2005, 2011] (2005, green squares and 2011, blue squares). The shaded area between both curves represents, *in fine*, the possible range of the simulated transport. Red-contoured triangles represent the main records of geodynamic and oceanic events.

reached half of its present-day transport (67 Sv) during the late Oligocene (Figure 8).

4. Conclusion

[18] The ACC has long been considered as a major actor of the climate of the southern high latitudes. The assertion rested on the blocking role of the ACC that prevents the warm surface waters from subtropical gyres from reaching Antarctica. Our results indicate that the development of the ACC is a consequence of the Cenozoic global cooling. In details, radiative cooling of the seawater surrounding Antarctica would have generated an increase in the sea-ice cover and the steepening of the latitudinal density distribution. These changes in the physical properties of the Southern Ocean would in turn have favored the onset of a mature ACC but causes and consequences are always difficult to ascribe within a fully coupled model [*Gent et al.*, 2001; *Gnanadesikan and Hallberg*, 2000]. Our model results favor the ACC as a consequence of climate changes. This does not close the door for a feedback effect of the ACC on climate, either directly as envisioned by *Toggweiler and Bjornsson* [2000] or indirectly through an increase in primary production in the Southern Ocean that would have lowered the atmospheric CO_2 concentration [*Scher and Martin*, 2006].

[19] **Acknowledgments.** This work was funded by the 'Agence Nationale de la Recherche' (ANR, COLORS project). We thank Gilles Ramstein and three anonymous reviewers for their helpful comments and discussions.

References

Arzel, O., T. Fichefet, and H. Goosse (2006), Sea Ice evolution over the 20th and 21st centuries as simulated by current AOGCMs, *Ocean Modell.*, *12*, 401–415, doi:10.1016/j.ocemod.2005.08.002.

Barker, P. F., and E. Thomas (2004), Origin, signature and palaeoclimatic influence of the Antarctic Circumpolar Current, *Earth Sci. Rev.*, *66*(1–2), 143–162, doi:10.1016/j.earscirev.2003.10.003.

Barrier, E., and B. Vrielynck (2008), *Palaeotectonic Maps of the Middle East*, Comm. for the Geol. Map of the World, Paris.

Bettge, T. W., J. W. Weatherly, W. M. Washington, D. Pollard, B. P. Briegleb, and W. G. Strand Jr. (1996), The CSM Sea Ice Model, *NCAR Tech. Note NCAR/TN-425+STR*, Nat. Cent. for Atmos. Res, Boulder, Colo.

Bice, K. L., E. J. Barron, and W. H. Peterson (1998), Reconstruction of realistic Early Eocene paleobathymetry and ocean GCM sensitivity to specified basin configuration, in *Tectonic Boundary Conditions for Climate Reconstruction*, edited by T. Crowley and K. Burke, pp. 227–247, Oxford Univ. Press, Oxford, U. K.

Cai, W. J., and P. G. Baines (1996), Interactions between thermohaline- and wind-driven circulations and their relevance to the dynamics of the Antarctic Circumpolar Current, in a coarse-resolution global ocean general circulation model, *J. Geophys. Res.*, *101*(C6), 14,073–14,093, doi:10.1029/96JC00669.

Cunningham, S. A., S. G. Alderson, B. A. King, and M. A. Brandon (2003), Transport and variability of the Antarctic Circumpolar Current in Drake Passage, *J. Geophys. Res.*, *108*(C5), 8084, doi:10.1029/2001JC001147.

DeConto, R. M., and D. Pollard (2003), Rapid Cenozoic glaciation of Antarctica induced by declining atmospheric CO_2, *Nature*, *421*(6920), 245–249, doi:10.1038/nature01290.

Dera, G., and Y. Donnadieu (2012), Modelling evidences for global warming, Arctic seawater freshening, and sluggish oceanic circulation during the Early Toarcian anoxic event, *Paleoceanography*, *27*, PA2211, doi:10.1029/2012PA002283.

Donnadieu, Y., Y. Goddéris, and N. Bouttes (2009), Exploring the climatic impact of the continental vegetation on th Mesozoic atmospheric CO_2 and climate history, *Clim. Past*, *5*, 85–96, doi:10.5194/cp-5-85-2009.

Ehrmann, W. U., and A. Mackensen (1992), Sedimentological evidence for the formation of an east Antarctic ice-sheet in Eocene Oligocene time, *Palaeogeogr. Palaeoclimatol. Palaeoecol.*, *93*(1–2), 85–112, doi:10.1016/0031-0182(92)90185-8.

Firing, Y. L., T. K. Chereskin, and M. R. Mazloff (2011), Vertical structure and transport of the Antarctic Circumpolar Current in Drake Passage from direct velocity observations, *J. Geophys. Res.*, *116*, C08015, doi:10.1029/2011JC006999.

Gent, P. R., W. G. Large, and F. O. Bryan (2001), What sets the mean transport through Drake Passage?, *J. Geophys. Res.*, *106*(C2), 2693–2712, doi:10.1029/2000JC900036.

Gloersen, P., W. J. Campbell, D. J. Cavalieri, J. C. Comiso, C. L. Parkinson, and H. J. Zwally (1992), Satellite passive microwave observation and analysis of Arctic and Antarctic sea ice, 1978–1987, *Ann. Glaciol.*, *17*, 149–154.

Gnanadesikan, A., and R. W. Hallberg (2000), On the relationship of the Circumpolar Current to Southern Hemisphere winds in coarse-resolution ocean models, *J. Phys. Oceanogr.*, *30*(8), 2013–2034, doi:10.1175/1520-0485(2000)030<2013:OTROTC>2.0.CO;2.

Holland, M. M., and M. N. Raphael (2006), Twentieth century simulation of the southern hemisphere climate in coupled models. Part II: Sea ice conditions and variability, *Clim. Dyn.*, *26*, 229–245, doi:10.1007/s00382-005-0087-3.

Huber, M., and D. Nof (2006), The ocean circulation in the southern hemisphere and its climatic impacts in the Eocene, *Palaeogeogr. Palaeoclimatol. Palaeoecol.*, *231*(1–2), 9–28, doi:10.1016/j.palaeo.2005.07.037.

Huber, M., and L. C. Sloan (2001), Heat transport, deep waters and thermal gradients: Coupled simulation of an Eocene "greenhouse" climate, *Geophys. Res. Lett.*, *28*, 3481–3484, doi:10.1029/2001GL012943.

Huber, M., L. C. Sloan, and C. Shellito (2003), Early Paleogene oceans and climate: A fully coupled modeling approach using the NCAR CCSM, in *Causes and Consequences of Globally Warm Climate in the Early Paleogene*, edited by S. L. Wing et al., *Geol. Soc. Spec. Publ.*, *369*, 25–47.

Huber, M., H. Brinkhuis, C. E. Stickley, K. Doos, A. Sluijs, J. Warnaar, S. A. Schellenberg, and G. L. Williams (2004), Eocene circulation of the Southern Ocean: Was Antarctica kept warm by subtropical waters?, *Paleoceanography*, *19*, PA4026, doi:10.1029/2004PA001014.

Iturralde-Vinent, M. A., and R. D. E. MacPhee (1999), Paleogeography of the Caribbean region: Implications for cenozoic biogeography, *Bull. Am. Mus. Nat. Hist.*, *238*, 1–95.

Jacob, R. (1997), Low frequency variability in a simulated atmosphere ocean system, PhD thesis, Univ. of Wis.-Madison, Madison.

Katz, M. E., B. S. Cramer, J. R. Toggweiler, G. Esmay, C. J. Liu, K. G. Miller, Y. Rosenthal, B. S. Wade, and J. D. Wright (2011), Impact of Antarctic Circumpolar Current development on Late Paleogene ocean structure, *Science*, *332*(6033), 1076–1079, doi:10.1126/science.1202122.

Kennett, J. P. (1977), Cenozoic evolution of Antarctic glaciation, the Circum-Antarctic Ocean, and their impact on global paleoceanography, *J. Geophys. Res.*, *82*(27), 3843–3860, doi:10.1029/JC082i027p03843.

Kennett, J. P., et al. (1974), Development of Circum-Antarctic Current, *Science*, *186*(4159), 144–147, doi:10.1126/science.186.4159.144.

Kiehl, J. T., J. J. Hack, G. B. Bonan, B. A. Boville, B. P. Briegleb, D. L. Williamson, and P. J. Rasch (1996), Description of the NCAR Community Climate Model (CCM3), *NCAR Tech. Note NCAR/TN-420+STR*, 152 pp., Natl. Cent. for Atmos. Res, Boulder, Colo.

Lagabrielle, Y., Y. Goddéris, Y. Donnadieu, J. Malavieille, and M. Suarez (2009), The tectonic history of Drake Passage and its possible impacts on global climate, *Earth Planet. Sci. Lett.*, *279*, 197–211, doi:10.1016/j.epsl.2008.12.037.

Livermore, R., A. Nankivell, G. Eagles, and P. Morris (2005), Paleogene opening of Drake Passage, *Earth Planet. Sci. Lett.*, *236*(1–2), 459–470, doi:10.1016/j.epsl.2005.03.027.

Lyle, M., S. Gibbs, T. C. Moore, and D. K. Rea (2007), Late Oligocene initiation of the Antarctic circumpolar current: Evidence from the South Pacific, *Geology*, *35*(8), 691–694, doi:10.1130/G23806A.1.

Mikolajewicz, U., E. Maier-Reimer, T. J. Crowley, and K. Y. Kim (1993), Effect of Drake Passage and panamian gateways on the circulation of an ocean model, *Paleoceanography*, *8*, 409–426, doi:10.1029/93PA00893.

Munk, W. H., and E. Palmen (1951), Note on the dynamics of the Antarctic Circumpolar Current, *Tellus*, *3*, 53–55, doi:10.1111/j.2153-3490.1951.tb00776.x.

Murphy, M. G., and J. P. Kennett (1986), Development of latitudinal thermal-gradients during the Oligocene: Oxygen-isotope evidence from the southwest Pacific, *Initial Rep. Deep Sea Drill. Proj.*, *90*, 1347–1360.

Nong, G. T., R. G. Najjar, D. Seidov, and W. H. Peterson (2000), Simulation of ocean temperature change due to the opening of Drake Passage, *Geophys. Res. Lett.*, *27*, 2689–2692, doi:10.1029/1999GL011072.

Pagani, M., J. C. Zachos, K. H. Freeman, B. Tipple, and S. Bohaty (2005), Marked decline in atmospheric carbon dioxide concentrations during the Paleogene, *Science*, *309*, 600–603, doi:10.1126/science.1110063.

Pagani, M., M. Huber, Z. H. Liu, S. M. Bohaty, J. Henderiks, W. Sijp, S. Krishnan, and R. M. DeConto (2011), The role of carbon dioxide during the onset of Antarctic Glaciation, *Science*, *334*(6060), 1261–1264, doi:10.1126/science.1203909.

Pfuhl, H. A., and I. N. McCave (2005), Evidence for late Oligocene establishment of the Antarctic Circumpolar Current, *Earth Planet. Sci. Lett.*, *235*(3–4), 715–728, doi:10.1016/j.epsl.2005.04.025.

Poulsen, C. J., and R. L. Jacob (2004), Factors that inhibit snowball Earth simulation, *Paleoceanography*, *19*, PA4021, doi:10.1029/2004PA001056.

Roche, D. M., X. Crosta, and H. Renssen (2012), Evaluating Southern Ocean sea-ice for the Last Glacial Maximum and pre-industrial climates: PMIP-2 models and data evidence, *Quat. Sci. Rev.*, in press.

Russell, J. L., R. J. Stouffer, and K. W. Dixon (2006), Intercomparison of the Southern Ocean circulations in IPCC coupled model control simulations, *J. Clim.*, *19*(18), 4560–4575, doi:10.1175/JCLI3869.1.

Scher, H. D., and E. E. Martin (2006), Timing and climatic consequences of the opening of Drake Passage, *Science*, *312*(5772), 428–430, doi:10.1126/science.1120044.

Scher, H. D., and E. E. Martin (2008), Oligocene deep water export from the North Atlantic and the development of the Antarctic Circumpolar Current examined with neodymium isotopes, *Paleoceanography*, *23*, PA1205, doi:10.1029/2006PA001400.

Scotese, C. R. (2001), PALEOMAP digital map archive [CD-ROM], PALEOMAP Proj., Arlington, Tex.

Semtner, A. J. (1976), A model for the thermodynamic growth of sea ice in numerical investigations of climate, *J. Atmos. Sci.*, *6*, 379–389.

Sijp, W. P., and M. H. England (2004), Effect of the Drake Passage throughflow on global climate, *J. Phys. Oceanogr.*, *34*, 1254–1266, doi:10.1175/1520-0485(2004)034<1254:EOTDPT>2.0.CO;2.

Sijp, W. P., and M. H. England (2005), On the role of the Drake Passage in controlling the stability of the ocean's thermohaline circulation, *J. Clim.*, *18*, 1957–1966, doi:10.1175/JCLI3376.1.

Sijp, W. P., M. H. England, and R. J. Toggweiler (2009), Effect of ocean gateway changes under greenhouse warmth, *J. Clim.*, *22*, 6639–6652, doi:10.1175/2009JCLI3003.1.

Sijp, W. P., M. H. England, and M. Huber (2011), Effect of the deepening of the Tasman Gateway on the global ocean, *Paleoceanography*, *26*, PA4207, doi:10.1029/2011PA002143.

Stickley, C. E., H. Brinkhuis, S. A. Schellenberg, A. Sluijs, U. Rohl, M. Fuller, M. Grauert, M. Huber, J. Warnaar, and G. L. Williams (2004), Timing and nature of the deepening of the Tasmanian Gateway, *Paleoceanography*, *19*, PA4027, doi:10.1029/2004PA001022.

Stommel, H. (1957), A survey of ocean current theory, *Deep Sea Res.*, *4*(3), 149–184.

Toggweiler, J. R., and H. Bjornsson (2000), Drake Passage and palaeoclimate, *J. Quat. Sci.*, *15*(4), 319–328, doi:10.1002/1099-1417(200005)15:4<319::AID-JQS545>3.0.CO;2-C.

Toggweiler, J. R., J. L. Russell, and S. R. Carson (2006), Midlatitude westerlies, atmospheric CO_2, and climate change during the ice ages, *Paleoceanography*, *21*, PA2005, doi:10.1029/2005PA001154.

Weatherly, J. W., B. P. Briegleb, W. G. Large, and J. A. Maslanik (1998), Sea ice and polar climate in the NCAR CSM, *J. Clim.*, *11*, 1472–1486, doi:10.1175/1520-0442(1998)011<1472:SIAPCI>2.0.CO;2.

Whitworth, T., III, and R. G. Peterson (1985), Volume transport of the Antarctic Circumpolar Current from bottom pressure measurements, *J. Phys. Oceanogr.*, *15*, 810–816, doi:10.1175/1520-0485(1985)015<0810:VTOTAC>2.0.CO;2.

Wilson, G. S., A. P. Roberts, K. L. Verosub, F. Florindo, and L. Sagnotti (1998), Magnetobiostratigraphic chronology of the Eocene-Oligocene transition in the CIROS-1 core, Victoria Land margin, Antarctica: Implications for Antarctic glacial history, *Geol. Soc. Am. Bull.*, *110*(1), 35–47, doi:10.1130/0016-7606(1998)110<0035:MCOTEO>2.3.CO;2.

Zachos, J. C., T. M. Quinn, and K. A. Salamy (1996), High-resolution (10^4 years) deep-sea foraminiferal stable isotope records of the Eocene-Oligocene climate transition, *Paleoceanography*, *11*(3), 251–266, doi:10.1029/96PA00571.

Zachos, J. C., B. N. Opdyke, T. M. Quinn, C. E. Jones, and A. N. Halliday (1999), Early cenozoic glaciation, antarctic weathering, and seawater $^{87}Sr/^{86}Sr$: Is there a link?, *Chem. Geol.*, *161*(1–3), 165–180, doi:10.1016/S0009-2541(99)00085-6.

Zachos, J. C., M. Pagani, L. Sloan, E. Thomas, and K. Billups (2001), Trends, rhythms, and aberrations in global climate 65 Ma to present, *Science*, *292*, 686–693, doi:10.1126/science.1059412.

Zhang, Z.-S., Q. Yan, and H.-J. Wang (2010), Has the Drake passage played an essential role in the Cenozoic cooling?, *Atmos. Oceanic Sci. Lett.*, *3*(5), 288–292.